

Surface Enrichment in Polystyrene/Poly(vinyl methyl ether) Blends. 3. An Analysis of the Near-Surface Composition Profile

J. M. G. Cowie,* B. G. Devlin, and I. J. McEwen

Department of Chemistry, Heriot-Watt University, Edinburgh, Scotland EH14 4AS

Received February 18, 1992; Revised Manuscript Received June 29, 1993*

ABSTRACT: An expression is developed to express experimental ATR infrared absorbance ratios arising from surface enrichment in poly(vinyl methyl ether) (PVME)/polystyrene (PS) blends. Blend surfaces are enriched with PVME, which has the lower surface energy, and are found to have a characteristic depth of order 0.25×10^{-6} m. The effect of stabilizing the blends by hydrogen bonding leads to a reduction in surface enrichment. The surface excess is also calculated using a simplified mean-field approach, and these are compared with experiment. The limitations of ATR spectroscopy for surface studies are highlighted.

Introduction

The advent of Fourier transform techniques has brought about something of a renaissance in the vibrational spectroscopy of polymers, most especially of solid samples which can only be examined in reflectance which gives inherently low signal levels at the detector. Fourier transform infrared attenuated total reflectance (FTIR-ATR) studies are now a matter of simple routine. Since this technique relies on the coupling of an internally reflected beam with a sample in physical contact with the reflecting interface, it returns information on the number of absorbing species close to the surface. The purist may be disinclined to regard FTIR-ATR as a "true" surface technique since the sampling depth is on the order of $(1-3) \times 10^{-6}$ m (compared, for example, with X-ray photoelectron spectroscopy (XPS) which samples the topmost 6×10^{-9} m). Indeed in many applications the information obtained is reasonably regarded as representative of the bulk. However, where the surface structure extends significantly into the bulk, differences between a reflectance spectrum and the corresponding transmission spectrum may be expected.

In the first two papers in this series we reported the use of FTIR-ATR to characterize the surfaces of poly(vinyl methyl ether)/polystyrene (PVME/PS) single-phase blends^{1,2} in which the apparent surface volume fraction of PVME was found to be measurably in excess of the bulk composition. These results parallel findings from XPS and surface tension measurements^{3,4} which also indicated the surface to be enriched in the lower surface energy component (PVME). By introducing specific intermolecular hydrogen-bonding structures, the surface enrichment was demonstrated to respond to changes in the balance between surface and bulk thermodynamics.² When the blend heat of mixing became sufficiently negative (about -3 J cm^{-3}), there was no longer a measurable surface excess of PVME.

In reaching these conclusions we were careful to point out the semiquantitative nature of the results. The ATR technique can be considered to integrate over a subsurface depth which may be described in terms of an equivalent thickness in a transmission experiment.⁵ Since this is typically on the order of 10^{-6} m, there is obviously a limit to its usefulness in determining the presence or absence of a surface excess. For example, it is most unlikely that monolayer coverages can be detected in any normal ATR

experiment. In this paper we quantify more precisely the surface excess of PVME in PVME/PS blends as found by ATR spectroscopy and attempt to relate these findings to the predictions of current mean-field theory.

Theoretical Background

The theoretical aspects and practical applications of reflectance spectroscopy are comprehensively covered by Harrick.⁵ The reflectivity R of a surface is defined as the ratio of the intensity of the reflected beam to that of the incident beam. The absorption parameter (α) for a single reflection is simply $(1 - R)$. The internally reflected radiation does not itself penetrate beyond the reflecting interface, but the evanescent electric field set up in the sample may couple with optically absorbing species such that $R < 1$. The evanescent field intensity at a distance z from the surface is given by^{5,6}

$$E^2 = E_0^2 \exp(-\alpha z) \quad (1)$$

where

$$\alpha = (2/dp + n_{21}\epsilon C) \quad (2)$$

E_0^2 is the field strength at the surface, and dp is the "depth of penetration" as defined by Harrick.⁵ The extinction coefficient and concentration of the absorbing species are ϵ and C , respectively. n_{21} is the ratio of the refractive index of the internal reflection element to that of the sample. The second term on the right-hand side of eq 2 quantifies intensity attenuation due to Beer's law absorption, and the first term is the unperturbed exponential decay of the evanescent field.

The concept of an equivalent thickness is no longer useful, nor indeed mathematically valid, if the distribution of the absorbing species within the subsurface is nonuniform. Here C must be expressed as an appropriate concentration profile $C(z)$ and α also becomes a function of z , $\alpha(z)$. For weak absorptions the amount of radiation absorbed is proportional to the intensity at the point of absorption,⁵ the absorption parameter for an absorbing species "i" is obtained from the integral⁶

$$a_i = (n_{21}E_0^2/\cos \theta) \int_0^\infty [\epsilon_i C_i(z) \exp(-\int_0^z \alpha_i(z) dz)] dz \quad (3)$$

Expression (3) is mathematically somewhat cumbersome, but it adequately suits our purpose to simplify matters by employing α_i as defined in eq 2 in place of $\alpha_i(z)$. θ is the incident angle at the interface.

* Abstract published in *Advance ACS Abstracts*, September 1, 1993.

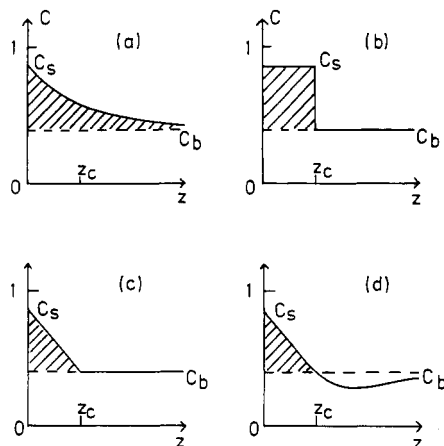


Figure 1. Schematics of various surface enrichment profiles. The surface volume fraction is C_s ; the bulk volume fraction is C_b and is indicated by a broken line. Hatched areas are integrated surface excesses z^* . Exponential (a), step (b), linear (c), critically damped sine (d).

The concentration profile may be expressed in a perfectly general manner by

$$C_i(z) = C_{bi} + (C_{si} - C_{bi})g(z/z_c) \quad (4)$$

Here C_{si} is the surface concentration of species i , and this decays according to some function of distance $g(z/z_c)$ toward the bulk value C_{bi} , as illustrated schematically in Figure 1. The constant z_c is the characteristic parameter of the profile. For example, if the profile is exponential, then z_c is the distance at which $C_{si} - C_{bi}$ is $1/e$ of its initial value. Changing the variable by setting $x = z/z_c$ and collecting optical constants as $\beta_i = n_{21}^2 E_0^2 \epsilon_i / \cos \theta$ enables eq 3 to be reexpressed as

$$a_i = \beta_i z_c C_{bi} \int_0^\infty \exp(-xz_c \alpha_i) dx + \beta_i z_c (C_{si} - C_{bi}) \int_0^\infty g(x) \exp(-xz_c \alpha_i) dx \quad (5)$$

It is convenient to introduce a surface enrichment index $f_i = (C_{si} - C_{bi})/C_{bi}$, which defines the excess surface concentration in terms of the bulk concentration, and to set $k_i = \alpha_i z_c$. Integration of eq 5 then yields

$$\alpha_i = (\beta_i C_{bi} / \alpha_i) [1 + f_i \{k_i \int_0^\infty g(x) \exp(-k_i x) dx\}] \quad (6)$$

The term preceding the square brackets is the absorption from a uniform concentration of absorbing species C_{bi} , while the term within the braces quantifies the increase in absorption from the excess surface concentration profile.

Equation 6 expresses all the limitations of reflectance spectroscopy when confronted with concentration profiles. The absorption intensity depends on three (invariably) unknown parameters, surface concentration C_{si} , characteristic length z_c , and the correct form of the decay function $g(x)$. The integral within the braces is the Laplace transform of $g(x)$, which, in principle, can generate a unique function $g(x)$ from absorption data obtained at different angles of incidence since dp is a function of θ and so $k_i = k_i(\theta)$. In practice it is unlikely that data of sufficient quality can be realized, and even so a value for C_{si} must be chosen. With this as a pragmatic constraint we proceed by assuming a profile $g(x)$ and find that expression (6) reduces to quite manageable forms for a number of profiles, as can be seen from inspection of Table I where the term in braces has been evaluated for various $g(x)$. On the basis that the perturbing action of a surface falls off progressively with distance, then logically $g(x)$ should be a monotonic function. One sensible choice of the profile is consequently

Table I. Integral Term of Equation 6 Evaluated for Various Surface Profiles $g(x)$

profile	$g(x)$	range of x	$\{k_i \int_0^\infty g(x) \exp(-k_i x) dx\}$
exponential	$\exp(-x)$	$0 \leq x < \infty$	$k_i / (1 + k_i)$
step	1	$0 \leq x \leq 1$	$(1 - \exp(-k_i))$
	0	$x > 1$	
linear	$(1 - x)$	$0 \leq x \leq 1$	$[1 - (1/k_i)(1 - \exp(-k_i))]$
damped sine	$(1 - x)/\exp(x)$	$0 \leq x \leq 1$	$k_i^2 / (1 + k_i^2)$

$g(x) = \exp(-x)$ which leads to a particularly simple form of eq 6.

Here we are considering binary blends containing two species, i and j , where an excess of i at the surface automatically implies a depletion of j . The absorption parameter for species j is also described by eq 6, but with i replaced by j and with the term in the square brackets expressed as a difference rather than a sum. The overall absorption due to j is thus less than that from a uniform distribution of this species.

Experimental Section

Both PS and PVME samples were obtained from Polysciences; M_n values were 575×10^3 and 51×10^3 , respectively. The synthesis of styrene copolymers containing a hydroxyl functionality and blend preparation have all been described previously.^{1,2}

Transmission spectra and ATR spectra of the polymer-air interfaces of PS/PVME blends were obtained using a Perkin-Elmer 1720X FTIR spectrometer and a Spectra-Tech 302 ATR attachment. The aromatic deformation mode at 699 cm^{-1} and the ether stretching mode at 1084 cm^{-1} were used to characterize the relative amounts of PS and PVME, respectively, in miscible blends of the two polymers. The extinction coefficients for these have been determined¹ as $\epsilon_{\text{PS}} = 0.11 \times 10^6 \text{ m}^{-1}$ and $\epsilon_{\text{PVME}} = 0.089 \times 10^6 \text{ m}^{-1}$ (these are in the range suggested by Harrick⁵ within which the weak absorption approximations, and consequently eq 5, are valid). The ATR element was a $50 \text{ mm} \times 3 \text{ mm}$ KRS prism with a face angle of 45° (giving a nominal 13 internal reflections). The average refractive index for KRS (n_1) is 2.40 in the infrared region, and the angle of incidence for internal reflection (θ) was 51.2° . The refractive index of a polymer blend (n_2) was taken as the volume fraction average of the refractive indices of PS and PVME.⁷ The values of dp are calculated for this system as before,^{1,2} at 1084 cm^{-1} dp is $1.33 \times 10^{-6} \text{ m}$ and at 699 cm^{-1} dp is $2.04 \times 10^{-6} \text{ m}$.

ATR-Determined Surface Excesses for PVME/PS Blends

Equation 6 predicts the absorption for a single reflection; for N reflections the instrumental absorbance (A) is related to the absorption parameter by $-A/N = \log(1 - a) \approx -a/2.303$ for small values of a . The compliant nature of the samples allowed good intimate contact with the ATR element; even so it has been demonstrated that by using band ratios accurate quantitative data are obtained⁸ and so it follows that $A_i/A_j \approx a_i/a_j$. Setting PVME as i and PS as j , absorbing at 1084 and 699 cm^{-1} , respectively, and after some algebra, eq 6 can be used to express the ratio of the experimental absorbances $R_a = A_{\text{PVME}}/A_{\text{PS}} \approx a_{\text{PVME}}/a_{\text{PS}}$ for an assumed exponential profile as

$$R_a = R_c \frac{1 + f_{\text{PVME}}[k_{\text{PVME}}/(1 + k_{\text{PVME}})]}{1 - f_{\text{PS}}[k_{\text{PS}}/(1 + k_{\text{PS}})]} \quad (7)$$

where

$$k_{\text{PS}} = k_{\text{PVME}}(\alpha_{\text{PS}}/\alpha_{\text{PVME}}) \quad (8)$$

$$f_{\text{PS}} = f_{\text{PVME}}(C_{b,\text{PVME}}/C_{b,\text{PS}}) \quad (9)$$

and

$$R_c = C_{b,\text{PVME}}\epsilon_{\text{PVME}}\alpha_{\text{PS}}/C_{b,\text{PS}}\epsilon_{\text{PS}}\alpha_{\text{PVME}} \quad (10)$$

The ratio R_c , where the C_i in volume fractions, is numerically equal to R_a when surface enrichment is absent.

Table II. Experimental Values of the Ratios of Absorbances at 1084 and 699 cm^{-1} (R_a) for PS/PVME Blends, the Corresponding Characteristic Length (z_c), and Integrated Surface Excess (z^*) of an Assumed PVME Exponential Surface Profile

$C_{b,\text{PVME}}$	R_a (std dev)	R_c^a	$10^6 z_c/m$ (std dev)	$10^6 z^*/m$ (std dev)
0.90	3.26 (0.55)	4.63	-0.04 (0.02) ^b	-0.04 (0.02) ^b
0.75	1.54 (0.19)	1.57	0.02 (0.05)	0.00 (0.02)
0.50	0.85 (0.10)	0.54	0.26 (0.08)	0.13 (0.04)
0.25	0.35 (0.06)	0.19	0.18 (0.07)	0.14 (0.05)
0.10	0.30 (0.07)	0.063	0.31 (0.09)	0.28 (0.09)

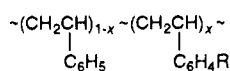
^a As defined by eq 9, $R_a = R_c$ when surface enrichment is absent.

^b Data for this blend indicate PS surface enrichment; a pure PS surface was assumed for the calculation.

Equation 7 is nonlinear in f_i and k_i , and so neither separate values of C_{si} and z_c nor indeed the integrated surface excess $z^* = (C_{si} - C_{bi})z_c$ can be obtained from measurements of the ratio R_a . It is necessary to assign a value to C_{si} and to solve for the corresponding value of z_c iteratively. In this present case we have set $C_{a,\text{PVME}}$ equal to unity (an assumption which we will return to later), modeling the blends as having a pure PVME surface decaying toward the bulk composition with characteristic decay length z_c . On this basis the values of z_c and z^* for a series of PS/PVME blends have been calculated and these are shown in Table II.

Each of the R_a values in Table II is the average of 6–8 measurements on separately prepared blends. There is quite a marked variation in this experimental parameter, and we can offer no clear reason why this is so, since aggregated instrumental and base-line reading errors should lead to a $\sim 3\%$ uncertainty in any absorbance value at the most. Most plausibly this scatter points to a variability between surfaces as prepared by the casting process, although care was always taken to reproduce the casting procedure. Nevertheless, the ATR data reveal significant PVME surface enrichment with increasing PS content, following the classical expectation based on surface tension differences.⁹

It is perhaps worth highlighting the limit of the ATR method at this juncture. The R_c entries in Table II are equivalent to experimental absorbance ratios when there is no surface excess. From these as a base line, the $\sim 3\%$ experimental uncertainty as noted above imposes a realistic lower detection limit on z^* of $\sim 0.004 \times 10^{-6}$ – 0.01×10^{-6} m for blend compositions in the range $C_{b,\text{PVME}} = 0.1$ – 0.5 . Surface enrichment levels below this must be regarded as effectively "invisible" to the technique. Equally, the rather high level of enrichment detected in the present system is well worth noting, in terms of the model chosen; apparently surface structures of $\sim 0.25 \times 10^{-6}$ m are present. The corresponding values of z^* for various PVME/(styrene copolymer) blends are compared with the homopolymer data in Figure 2. These copolymers contain low incorporations of the hydroxyl functionality para-substituted on the styrene units. The copolymer structures I–IV and abbreviations are given below, and their effect on blend stability as measured by the blend demixing temperatures has been reported in the preceding publication.²



$x = 0$ – 6 mol %

- | | |
|---|----------|
| I, R = OH | (4-HS) |
| II, R = $-\text{CH}(\text{CH}_3)\text{OH}$ | (4-HES) |
| III, R = $-\text{CH}(\text{CF}_3)\text{OH}$ | (4-TFHS) |
| IV, R = $-\text{C}(\text{CF}_3)_2\text{OH}$ | (4-HFHS) |

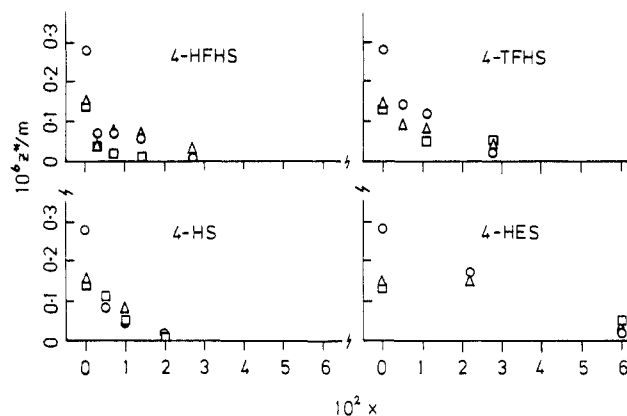


Figure 2. ATR-determined integrated surface excesses (z^*) for homopolymer PS/PVME blends and for copolymer/PVME blends at $C_{b,\text{PVME}} = 0.10$ (circles), 0.25 (triangles), and 0.50 (squares). x is the mole fraction of H-bonding units in the copolymer.

Briefly, the introduction of a small number of H-bonding sites results in an enhancement in blend stability but leaves surface forces unaffected. Blend surface free energy may still be lowered by placement of PVME at the surface; however, the maintenance of the necessary composition profile between surface and bulk is now thermodynamically less attractive and the overall effect of modifying PS/PVME blends in this way should be to reduce the near-surface enrichment by PVME. In quantitative terms a smaller integrated surface excess should result, and Figure 2 clearly shows this indeed to be the case. (Since comonomer compositions are restricted below 0.06 mole fraction, these data were calculated from eq 7 in the same manner as for homopolymer blends, but with the copolymer extinction coefficient given by $(1 - x)\epsilon_{\text{PS}}$.)

In each of the four copolymer blends z^* decays toward the limit of reliable detection with increasing (but small) degrees of H-bonding. Differing levels of effectiveness can be discerned from the figure; 4-HES and 4-TFHS (to a lesser extent) appear less able than 4-HFHS and 4-HS in stabilizing the blends against the formation of a surface excess. The next section discusses the formation of surface excesses in terms of a simplified mean-field theory.

Mean-Field Description of Surface Enrichment

The equilibrium surface composition and near-surface profile result from the minimization of the overall free energy, and this has been considered within the framework of the mean-field theory by Schmidt and Binder¹⁰ and also by Nakanishi and Pincus¹¹ on the basis of earlier treatments of the surface of liquid mixtures.^{12,13} Both take as their starting point an extended Flory–Huggins expression which accounts for spatially changing composition to which is added a contribution for the surface free energy. The resulting equations involve familiar lattice parameters but are somewhat complex. A simplification of this theory has recently been presented by Jones and Kramer¹⁴ for components of equal chain length (N). The surface composition is given in terms of a single reduced quantity (t), which measures the driving force for surface segregation, by

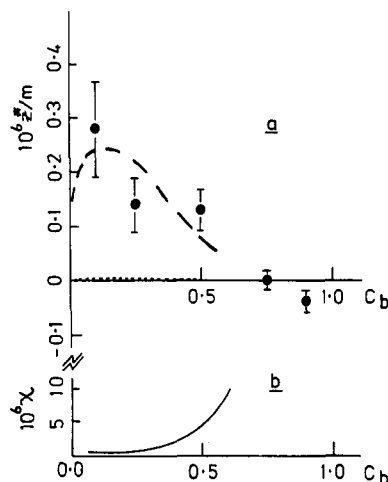
$$C_s = (C_b + t)/(1 + t) \quad (11)$$

The parameter t depends in turn on the two system parameters $\Delta\chi$ and $\Delta\gamma$. The latter is the difference in the surface energies of the components and the former the difference between the value of the segmental interaction and the value of the Flory parameter on the coexistence

Table III. Values of the Parameters Used to Calculate C_s and z^* for PS/PVME Blend Surfaces

param	value	ref
$\Delta\gamma/(\text{J m}^{-2})$	0.008	3
$b^3_{\text{PVME}}/10^{-28} \text{ m}^3$	0.787	15
$b^3_{\text{PS}}/10^{-28} \text{ m}^3$	1.41	15
$a_{\text{PS,PVME}}/10^{-10} \text{ m}$	7.0	14
$\chi_{\text{crit}}(\text{PS/PVME})$	0.0011	
$\chi_{\text{crit}}(\text{blends})^a$	0.0036	

^a The copolymer samples have molecular weights in the range 28×10^3 – 45×10^3 . A weighted average of 40×10^3 was used to calculate χ_{crit} .

**Figure 3.** ATR-determined integrated surface excesses (z^*) for homopolymer PS/PVME blends as a function of a PVME bulk volume fraction (a). Dotted line predicted with $\chi_{\text{S/VME}}$ equal to zero. Heavy broken line fitted as described in the text with $\chi_{\text{PS/PVME}}$ as shown in b.

boundary χ_b (i.e., $\Delta\chi = \chi_b - \chi_{\text{S/VME}}$). The expression for t is

$$t = (3b^3\Delta\gamma/akT)^2(1/\Delta\chi) \quad (12)$$

where T is the temperature, k is Boltzmann's constant, and a is the effective step length defined by the mean end-to-end distance, which, calculated from published data,¹⁵ turns out to be the same for both PS and PVME. The parameter b^3 is the volume of a Flory–Huggins lattice site and may be deduced for PS and PVME from the “hard-core” specific volumes given by Ougizawa, Dee, and Walsh,¹⁶ where we identify the lattice site volume as the hard-core segment volume. b^3 is taken as the volume fraction average in PS/PVME mixtures.

The magnitude of the segmental interaction parameter $\chi_{\text{S/VME}}$, characterizing the thermodynamic state of the bulk mixture, is a matter we have considered before.^{2,17,18} The system PS/PVME is best regarded as marginally miscible and can be considered as effectively athermal. Accepting this as a useful starting point, $\chi_{\text{S/VME}}$ is set equal to zero, and, with the other system parameters collected in Table III, C_s for PVME calculated via eq 11 is close to unity for all values of C_b .

The integrated surface excess z^* does not require the mathematical form of the surface profile to be known and may be obtained from the expression¹³

$$z^* = (a/3\Delta\chi)[\arcsin[(1 - C_b)^{1/2}] - \arcsin[(1 - C_s)^{1/2}]] \quad (13)$$

For PVME/PS homopolymer blends the values of z^* (PVME) predicted by eq 13 are fully 2 orders of magnitude less than those obtained experimentally (see Figure 3), in fact a level of surface enrichment not reliably detected by

Table IV. Enthalpies of H-Bond Formation, “ χ_{HB} ”, and Corresponding Calculated Surface Excesses for 25/75 by Volume PVME/PS Copolymer Blends

	$\Delta H_{\text{HB}}/(\text{kJ mol}^{-1})$	“ χ_{HB} ”	z^*/m
4-HES	-5	-0.060	8.5×10^{-10}
4-TFHS	-13	-0.156	4.3×10^{-10}
4-HS	-23	-0.276	2.8×10^{-10}
4-HFHS	-35	-0.420	2.0×10^{-10}

ATR methods according to our estimates above. Some remarks regarding this rather disappointing agreement between experiment and theory are required.

Equations 11 and 13 are not strictly applicable where the component degrees of polymerization are different, but this is an unavoidable approximation here since a formal generalization to the case of unequal chain lengths appears mathematically intractable. In another sense also we have strayed from the intended area of applicability. Expression (13) is the exact solution to a more general integral (for z^*) under the constraint that $|\chi_{i-j}N|$ is large. However, in this present case this proved relatively unimportant; unapproximated z^* values obtained by numerical integration are only 20% or so different from those obtained directly from eq 13, leaving the conclusion that surface separation in this system is considerably greater than might be predicted if enthalpy effects are assumed to be negligibly small.

The experimental trend of z^* with blend composition is well enough reproduced by eq 13 (and indeed also by numerical integration) if a composition-dependent $\Delta\chi$ ($\sim 5 \times 10^{-6}$) is used as shown in Figure 3. Granting this unashamed data fitting exercise an element of credence, the observed surface excesses imply that $\chi_{\text{S/VME}}$ is almost identical with χ_{crit} for the system; i.e., $\chi_{\text{S/VME}} \approx 0.0011$. Although this is a perfectly acceptable value, and well within the range of previous experimental determinations of the parameter,¹⁷ only a semiquantitative confirmation of the predictive aspects of the theory has been achieved, namely, that when binary blends are close to demixing ($\chi_{i-j} \approx \chi_{\text{crit}}$), surface segregation should be quite extensive—as indeed it is for this system.

The behavior of the copolymer systems shown in Figure 2 also follows qualitatively from eq 13, given the reasonable premise that the introduction of H-bonded sites in the blend leads to a more favorable overall segmental interaction. In the previous paper of this series we described the equilibrium between intra- and intermolecular association in these blends² in terms of the fraction of bonded comonomer VME units (α) and a representative equilibrium constant for H-bond formation ($K_{\text{HB}} \approx 10$). Equating expression (2) of the previous paper, which relates the heat of mixing to the enthalpy of H-bond formation (ΔH_{HB}), with Flory's prescription¹⁹ for the heat of mixing, we can readily translate ΔH_{HB} into

$$“\chi_{\text{HB}}” = \alpha x \Delta H_{\text{HB}}/RT C_b \quad (14)$$

with $\alpha = 0.8$ for $K_{\text{HB}} = 10$ and small values of x . Estimates of ΔH_{HB} were obtained from the infrared spectra of the blends² and, from these, values of “ χ_{HB} ” at $x = 0.01$ and $C_b = 0.25$ are shown in Table IV. Added to a value of $\chi_{\text{S/VME}} = 0.0011$ from above, these produce overall negative values of χ_{i-j} for the copolymer blends. The corresponding surface excesses according to eq 13, also shown in Table IV, are very much smaller than those observed. H-bond stabilization of PS/PVME blends against substantial surface segregation is thus far less effective than suggested by this application of the mean-field expressions.

This apparent discrepancy between the expected response of the blend systems, at least in a strictly quan-

Table V. Characteristic Distance and Integrated Excess for 10/90 vol % PVME/PS Homopolymer Blends Calculated for Various Profiles

profile	$10^6 z_c/m$		$10^6 z^*/m$	
	$C_s = 1$	$C_s = 0.75$	$C_s = 1$	$C_s = 0.75$
exponential	0.31	0.51	0.28	0.33
step	0.27	0.40	0.24	0.26
linear	0.56	0.87	0.25	0.28
damped sine	0.91	1.34	0.30	0.32

titative sense, may be a consequence of adding the nonrandom contribution of a highly specific interaction to the Flory parameter. Indeed the localized nature of the intercomponent interaction may provide the rationale for the observed behavior. The mean-field expressions are framed within the dimensional scale of several repeat units and, as seen above, predict characteristic dimensions, essentially of a (surface) phase-separated domain, on the order of a radius of gyration. Now the extent of the surface domain in PS/PVME is macroscopic, much more akin to that in "conventional" bulk two-phase systems. A strong interaction, if introduced at, say, the 1% level will only stabilize against phase separation locally. Only when such interactions are sufficiently numerous will the surface structures observed be noticeably affected. Nevertheless, a considerable measure of control over the extent of a surface segregated "layer" has been exerted by this modification to the blend thermodynamics, although the extent of this could not have been predicted *a priori* in the present system.

Other Profiles

To conclude, we return to the data in Table II for the PS/PVME homopolymer system. Values for z^* for other postulated forms for the surface profile are just as readily obtained from the ATR data using the alternative expressions given in Table I. These are shown for 10/90 vol % PVME/PS homopolymer blends in Table V, again assuming $C_s = 1.0$. Modeling the surface with either an exponential, a step, or a linear profile implies that the surface excess has been accrued by uniform depletion of PVME throughout the entire bulk of the sample, and this may be questioned on the basis of diffusion limitations. The last profile in the table describes a more localized process and uses the expression for a critically damped sine wave. The model here is of a surface-enriched region immediately followed by a depletion zone. This contains an equivalent excess of the other component, the majority of which is close to the surface excess although it decays exponentially throughout the entire bulk sample (see Figure 1). Since the ATR "probe" also samples a buried PS-rich region, this profile results in a surface excess of PVME with a larger z_c value in comparison with the other profiles.

The question of which of these, or indeed any other choice, is the "correct" profile cannot be answered from the data presented here, for the reasons already mentioned. It can be argued that the simple profiles are equally as reasonable as any involving an adjacent depletion layer if it is recalled that the films examined here were solvent-cast and that long-range PVME diffusion, at least during part of this process, may not be severely impeded. In this respect also FTIR-ATR characterization of surface enrichment has its limits. However, Table V shows that the integrated surface excess is reasonably model-insensitive. Neither is it overly sensitive to the value of C_s assumed; recalculated values of z^* are also shown in the table for $C_s = 0.75$ and are at most only 20% greater than for an assumed pure PVME surface. Well-developed surface enrichment, as here, can thus be sensibly quantified by an ATR-determined integrated surface excess z^* , even when (as will inevitably be the case) C_s and $g(x)$ are unknown, but are assumed to have some reasonable value and profile, respectively.

Acknowledgment. The authors thank ICI (Paints) for financial support (B.G.D.) and for invaluable contributions from Dr. R. Ferguson.

References and Notes

- Cowie, J. M. G.; Devlin, B. G.; McEwen, I. J. *Polymer* **1993**, *34*, 501.
- Part 2 of this series: Cowie, J. M. G.; Devlin, B. G.; McEwen, I. J. *Polymer*, in press.
- Batia, Q. S.; Pan, D. H.; Koberstein, J. T. *Macromolecules* **1988**, *21*, 2166.
- Pan, D. H.; Prest, W. M. *J. Appl. Phys.* **1985**, *58*, 2861.
- Harrick, N. J. *Internal Reflection Spectroscopy*; Wiley-Interscience: New York, 1967.
- Tompkins, H. G. *Appl. Spectrosc.* **1974**, *28*, 335.
- van Krevelin, D. W. *Properties of Polymers*; Elsevier Scientific Publishing Co.: Amsterdam, The Netherlands, 1976.
- Mirabella, F. M. *Spectroscopy* **1990**, *5*, 20.
- Wu, S. *Polymer Interface and Adhesion*; Marcel Dekker: New York, 1982.
- Schmidt, I.; Binder, K. *J. Phys. (Paris)* **1985**, *46*, 1631.
- Nakanishi, H.; Pincus, P. *J. Chem. Phys.* **1983**, *79*, 997.
- Cahn, J. W. *J. Chem. Phys.* **1977**, *66*, 3367.
- van der Waals, J. D. *Z. Phys. Chem.* **1894**, *13*, 657.
- Jones, R. A. L.; Kramer, E. J. *Polymer* **1993**, *34*, 115.
- Brandrup, J.; Immergut, E. J., Eds. *Polymer Handbook*; John Wiley and Sons: New York, 1975.
- Ougizawa, T.; Dee, G. T.; Walsh, D. J. *Macromolecules* **1991**, *24*, 3834.
- Cowie, J. M. G.; McEwen, I. J.; Nadvornik, L. *Macromolecules* **1990**, *23*, 5106.
- Cowie, J. M. G.; Fernandez, M. D.; Fernandez, M. J.; McEwen, I. J. *Eur. Polym. J.* **1992**, *28*, 145.
- Flory, P. J. *Principles of Polymer Science*; Cornell University Press: Ithaca, NY, 1953.